Chemical Physics 405 (2012) 161–166

Contents lists available at SciVerse ScienceDirect

Chemical Physics

journal homepage: www.elsevier.com/locate/chemphys

Physisorption to chemisorption transition of NO_2 on graphene induced by the interplay of SiO_2 substrate and van der Waals forces: A first principles study

Jiayu Dai [a,*], Jianmin Yuan [a,b]

[a] Department of Physics, College of Science, National University of Defense Technology, Changsha 410073, People's Republic of China
[b] State key laboratory of high performance computing, National University of Defense Technology, Changsha 410073, People's Republic of China

ARTICLE INFO

Article history:
Received 23 April 2012
In final form 18 July 2012
Available online 25 July 2012

Keywords:
Graphene
Adsorption
Substrate effect
Van der Waals
Density-functional theory

ABSTRACT

The effect of SiO_2 substrate and van der Waals interactions on the adsorption of NO_2 molecule on graphene is studied using density functional theory. Contrary to physisorption on suspended graphene, both physisorption and chemisorption phenomena can be found, which are mainly caused by the covalent C–O bonds, the broken symmetry, and the local corrugations induced by SiO_2. The electronic structures of the system are significantly influenced after NO_2 adsorption, enhancing the detection of NO_2. Interestingly, NO_2 induces magnetization into graphene, and the spin polarization locates mainly on carbon atoms of graphene. The barrier of the transition from physisorption to chemisorption is about 0.05 eV, and this "pseudo barrier" can be overcome by van der Waals interactions. This work explains the experiments of graphene as gas sensors with high sensitivity, and supports new applications for electronic, spintronic devices.

1. Introduction

People have been looking for good materials as gas sensors with high sensitivity for a long time. Graphene exhibits potential applications in this field because of its unique properties. After its successful fabrication [1,2], experiments have shown that graphene can be a good sensor for the gases such as NO_2 [3,4] and NH_3 [5] with high sensitivity. Basically, it is expected that the adsorption of gas molecules on the sensors is stable and the changes of the conductivity should be observable. However, most of gases are found physisorbed on suspended intrinsic graphene [6–8]. Although the physisorption can also change the conductivity of intrinsic graphene, the small adsorption energy and weak coupling between gases and graphene indicate the unstable configuration at room temperature and little change of electronic structure [7]. On the contrary, the dopants and defects in graphene can strongly enhance the adsorption of molecules on graphene [9–14], indicating that doped atoms and defects play important roles in the applications of graphene. Thus, defects, dopants, gases and atoms adsorption or electric field are usually considered as the explanation of the sensitive behaviors of gas molecules on graphene [8,9,11,13,15–20].

We have to notice that in most experiments, graphene is supported on a substrate such as Si/SiO_2 or SiC [2,3,5]. There were a lot of researches about the effect of substrate on the electronic structures of graphene. For example, SiC can induce a band gap [21–23] and magnetic moments [24] in graphene, making SiC-graphene a good material for the usage in electronic devices. Also, SiO_2 can affect the atomic, electronic and magnetic structures of graphene [25–29]. Furthermore, SiO_2 plays a significant role in the adsorption of water on graphene [30], indicating the necessity of the consideration of the environment. According to experiments [31–33], molecules such as NO_2 and F4-TCNQ can induce the metal-to-insulator transition in the substrate-graphene system, giving an evidence on the chemisorption of NO_2, which was never observed in previous theoretical studies. In particular, the significant charge transfer between graphene and NO_2 was observed recently [33], which should not happen in the physisorption process. Until now, there are few studies about the effect of substrate on the adsorption of molecules on graphene, even though it may give some new physics theoretically and discover good materials in the practical applications. Besides, a recent study shows that the van der Waals interaction is important for the molecule adsorption on graphene-SiO_2 system [34], spurring us to reconsider the new mechanism for the adsorption.

In this work, by using density functional theory (DFT), we study the atomic and electronic structures of graphene on the oxygen terminated (O-terminated) SiO_2 substrate, looking for the most stable configuration. SiO_2 induces eight C–O covalent bonds and a small band gap for graphene. Then, one NO_2 molecule is put on different sites on the graphene surface. In this way, one chemisorption site is found with a large adsorption energy and a short distance between C atoms and the NO_2 molecule, which are caused

* Corresponding author. Tel.: +86 731 84576016; fax: +86 731 84573231.
E-mail addresses: jydai@nudt.edu.cn (J. Dai), jmyuan@nudt.edu.cn (J. Yuan).

0301-0104/$ - see front matter © 2012 Elsevier B.V. All rights reserved.
http://dx.doi.org/10.1016/j.chemphys.2012.07.008

by the break of π bonds in graphene and the local corrugations induced by the substrate. Meantime, the electronic and magnetic structures are changed by the NO_2 adsorption, in agreement with previous experiments and giving some new and interesting physics. The energy barrier from the physisorption to chemisorption is about 0.05 eV, which can be overcome directly by the consideration of van der Waals interactions. This gives a direct evidence for the substrate-induced transition from physisorption to chemisorption of NO_2 on graphene.

2. Computational details

In order to simulate the adsorption of NO_2 on SiO_2-graphene surface, density-functional theory (DFT) calculations using the Perdew-Burke-Ernzerhof (PBE) [35] approximation to the exchange–correlation potential [36] are performed. Spin polarization is allowed in all cases so that the magnetic properties can be obtained, as implemented in the Quantum-ESPRESSO package [37]. A plane-wave basis set up to a kinetic energy cutoff of 30 Ry for the wavefunction and of 300 Ry for the charge density is used. Several previous studies have shown that the chemical reactivity and bonds for graphene layer on the O-terminated SiO_2 surface are stronger than that on silicon terminated SiO_2 surface [29], and O-terminated surface can induce more interesting electronic structures such as a band gap in graphene [25,26]. Thus, we focus on the O-terminated surface of SiO_2 in this work. Using a slab configuration, a triclinic supercell of the SiO_2-graphene-adsorbate system is modeled using supercell containing 32 carbon atoms (4×4 graphene), 72 substrate atoms ($2 \times 2 \times 2$ SiO_2(100) surface), and one NO_2 molecule. Here, we put C atoms on the top of eight oxygen atoms, which are shown to be the most stable sites [29] and, different from most previous theoretical studies, whose C atoms are a little further away from the oxygen atoms [25,26]. In addition, eight hydrogen atoms are used to passivate the top oxygen atoms when we study the effect of H-passivated oxygen atoms on gas adsorption. The supercell constructed in this work is shown in Fig. 1. The lattice parameters of $a = b$=9.826 Å, c = 32 Å, $\alpha = \beta$=90^0, γ = 120^0 are adopted. This supercell makes the lattice mismatch of the interface between graphene and SiO_2 less than 0.01%, which has been applied successfully in previous studies [25,26,29]. A $3 \times 3 \times 1$ Monkhorst–Pack [38] grid and Methfessel–Paxton [39] smearing of 0.01 Ry is used for the sample of Brillouin Zone, and a $7 \times 7 \times 2$ Monkhorst–Pack grid (and the tetrahedron method [40]) is used for the calculation of the band structure (density of states (DOS)). Atomic positions are optimized until the maximum force on any atom is less than 0.001 a.u. Larger energy cutoff, more k-points were tested but no significant difference was found. In addition, we studied the system of H-passivated bottom Si atoms of SiO_2 substrate, and there was no influence on the results of adsorption. The van der Waals interactions, successfully applied in a lot of systems, are implemented by the Dion (vdw-DF) [41,42] and correction (DFT-D) [43,44] scheme. In this work, we used the DFT-D correction for the consideration of van der Waals interactions, which has been shown to perform better with PBE functional.

In analyzing the results, the adsorption energy is defined as

$$E_a = E_t - E_{(SiO_2+graphene)} - E_{NO_2}, \quad (1)$$

where E_t is the total energy of SiO_2 + graphene + NO_2 system, $E_{(SiO_2+graphene)}$ is the energy of the substrate-graphene system, and E_{NO_2} is the energy of the isolated NO_2 molecule. The distance from the adsorbate to the graphene surface is calculated between the atom of the molecule nearest to graphene layer and the carbon atoms of the graphene.

When NO_2 is placed on the graphene surface, three adsorbed sites are considered: two close sites (A and B) on top of C atoms, and the center of a carbon hexagon (C). For NO_2 molecule, different orientations are also considered, i.e., N atom close to graphene (n), O atom close to graphene (o), and parallel to graphene surface (p). With these initial configurations, the features of NO_2 on SiO_2-graphene surface can be outlined clearly, and the mechanism of adsorption is expected to be explained in this way.

3. Results and discussion

3.1. Graphene on SiO_2

Firstly, we will discuss the results without van der Waals correction. The monolayer graphene is initially deposited at a distance of 2.0 Å. The optimal configuration is shown in Fig. 2(a). Because the carbon atoms are placed on the top of oxygen atoms of SiO_2, eight C–O bonds form and the chemical reactivity is also strong [29] induced by the dangling bonds of oxygen atoms. Local corrugations with a height of 0.53 Å appear in graphene sheet. The structural analysis shows that the lengths of eight C–O bonds are 1.49 Å for shorter bonds and 1.50 Å for longer bonds, which are longer than the C–O bonds calculated using local density approximation (LDA) exchange–correlation functional [25]. This is reasonable because LDA exchange–correlation functional is well known for its overestimated binding energy and underestimated bond length. However, it is worth noting that there are some differences on

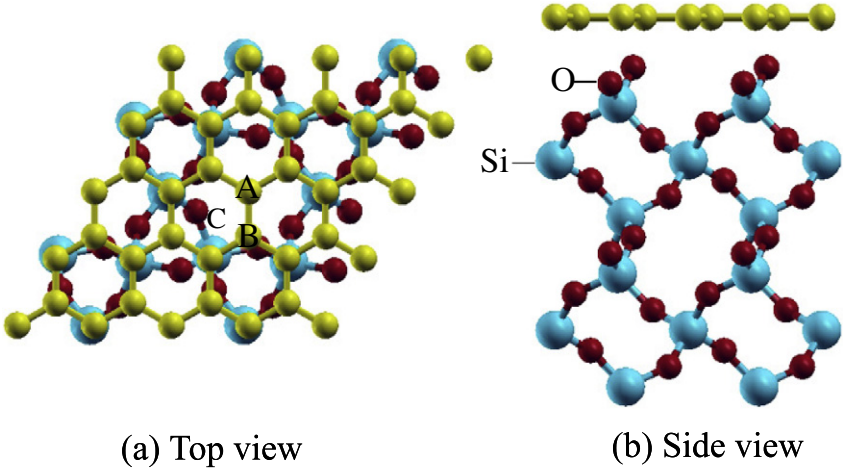

Fig. 1. Initial configurations of SiO_2-graphene system used in this work. (a) and (b) are the top and side views of the supercell. A–C are three sites for the adsorption of NO_2.

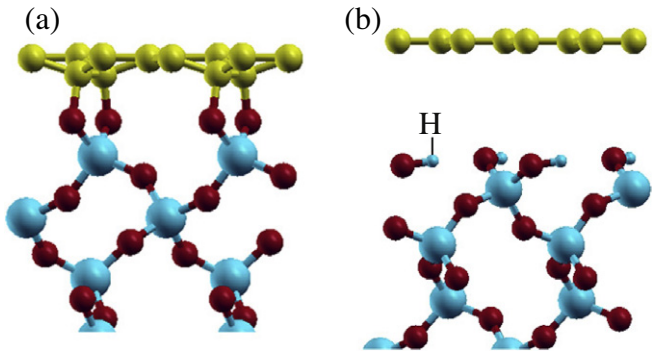

Fig. 2. Slices of final configurations of graphene on O-terminated SiO_2 surface (a), and graphene on O-terminated surface with H-passivation (b).

the atomic structures of graphene-SiO_2 interface here from the previous results [25,26]. For example, eight C–O covalent bonds are found in this work, compared with four C–O bonds in the previous report [25]. Thus, all eight surface oxygen atoms are in the same plane without significant recesses, which is more stable than the other interface structures [29]. Contrarily, the passivation of oxygen atoms at the interface between SiO_2 and graphene induces no bond formation, where the graphene layer is further away from the substrate with a distance of 3.91 Å, as shown in Fig. 2(b). Furthermore, the graphene layer is completely planar, and the length of OH bond is about 0.99 Å. Interestingly, the distance of OH···O hydrogen bond is 1.78 Å, which is in agreement with the bond length in water and water clusters [45]. The hydrogen bond network comparable to water indicates the strong structural stability for the configuration of H-passivated substrate.

Since the effect of O-terminated surface with H-passivation on graphene geometry is so different from that of the surface without H-passivated oxygen atoms, their electronic structures should be very different. As shown in Fig. 3, the covalent C–O bonds and local distortion of graphene induce dramatic changes for the electronic band structure, destroying the symmetry and spectrum of π bands in graphene and inducing a small band gap with a width of 0.06 eV. The previous results report larger band gaps for graphene-SiO_2 system, whose dominant reason is that the different adsorbed sites of graphene on SiO_2 surface and the different final interface structures. In the present work, eight C–O bonds are new reported structures, which eliminate all dangling bonds of oxygen. With this configuration, the SiO_2 surface exhibits its bulk properties, whose isolated band gap are large. On the other side, the π bands of graphene are strongly destroyed and the symmetry is broken. Thus, the cross band at Dirac point is separated with a small band gap shown. That is to say, the bands near Fermi level in Fig. 3 come from carbon in graphene. However, after H-passivated for oxygen atoms, the planar geometry of graphene is kept very well, and its semi-metal electronic structure, linear π bands, and Dirac point are also kept well, which are better than the results with LDA calculations [25]. Therefore, the graphene on O-terminated SiO_2 surface with H-passivation can be used to substitute the suspended graphene in experiments in order to investigate the properties of the intrinsic ideal graphene.

3.2. Adsorption of NO_2 without van der Waals

As discussed above, three sites shown in Fig. 1 for the adsorption of NO_2 with different molecular orientations are investigated. The results are collected in Table 1, where the adsorption energy, the distance between NO_2 and graphene surface (or the C–O, C–N bonds), and the magnetic moment of the system are shown. It is clear that NO_2 molecule is stably adsorbed on A site with a large adsorption energy and forming C–N or C–O bonds. For other sites and for all adsorption on H-passivated surface, NO_2 is obviously physisorbed with small adsorption energies and large distances from the graphene surface.

In Fig. 4, the charge densities of the typical chemisorption and physisorption are shown. For chemisorption, the charges of the NO_2 molecule and carbon atom in graphene are overlapped seriously, indicating the formation of chemical bonds. However, for physisorption, there is not any superposition appearing, showing

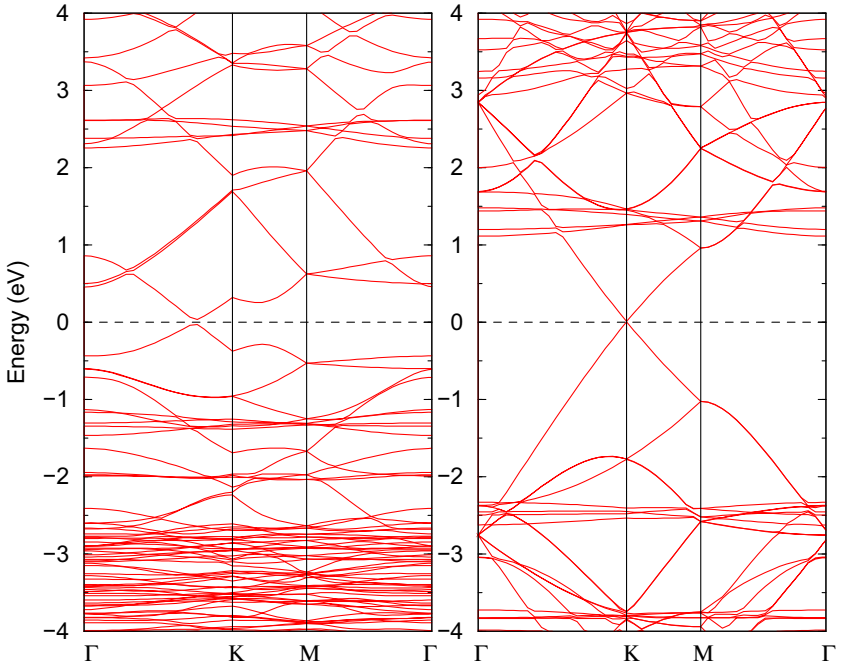

Fig. 3. Electronic band structures of graphene on O-terminated surface of SiO_2 substrate (left panel), and on the surface with H-passivation (right panel). Dashed lines represent the Fermi energy.

Table 1
Summary of the results of adsorption of NO_2 on SiO_2-graphene surface. The adsorption energy (E_a) and distance (d) with different adsorbed sites (S), different molecular orientation (T), and the magnetic moments (M_B) are shown. The data in brackets are the results of adsorption with H-passivated O-terminated surface.

S	T	E_a (eV)	d (Å)	M_B (μ_B)
A	n	−0.186 (−0.092)	1.633 (3.361)	1.02
	o	−0.160 (−0.085)	1.469 (3.352)	1.02
B	n	−0.070 (−0.059)	3.325 (3.362)	1.00
	o	−0.062 (−0.048)	3.344 (3.501)	1.00
C	n	−0.046 (−0.036)	2.958 (3.391)	1.00
	o	−0.017 (−0.033)	3.364 (3.432)	0.95
	p	−0.060 (−0.041)	3.012 (3.232)	0.98

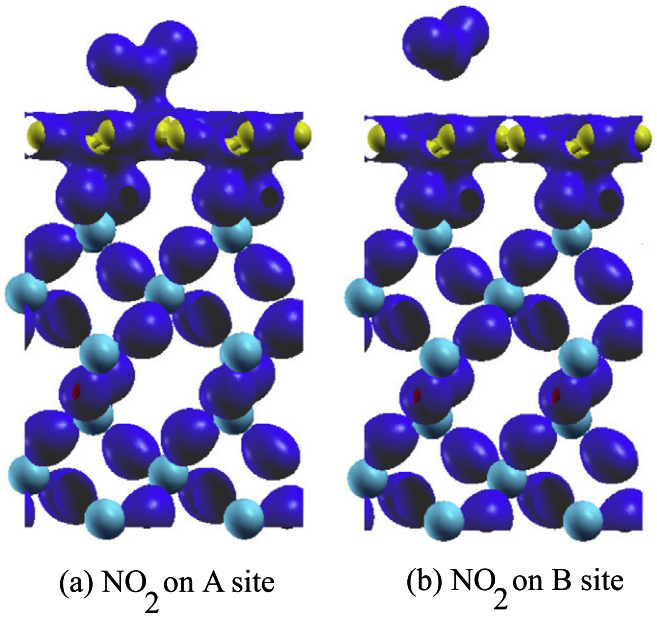

Fig. 4. (a) Charge density of "n" orientated NO_2 adsorption on A site; (b) Charge density of "n" orientated NO_2 adsorption on B site. Isosurface value is 0.1 a.u.

the decoupling between the molecule and the graphene surface. Furthermore, the formation of C–O bonds between the SiO_2 surface and graphene can be shown clearly in Fig. 4(a), where the charge densities of O atoms and C atoms are overlapped. Besides, in order to detect the NO_2 molecules with high sensitivity, the conductivity of the system after adsorption should change significantly. In Fig. 5, the DOSs for typical chemisorption and physisorption are shown. Comparing with the DOS of graphene-SiO_2 system without NO_2 adsorption, it is obvious that the DOS after chemisorption of NO_2 around Fermi level increases for both spin-up and spin-down electrons. Furthermore, it exhibits some characteristics of a half metal, whose DOS of spin-up electrons behaves as a semiconductor and spin-down electrons as a metal. This phenomenon should be stable due to the large adsorption energy. For the adsorption with H-passivation, although there is one peak appearing for the DOS of spin-down electrons, it would be unstable since the binding is very weak. The localized DOSs (LDOS) of NO_2 and C atoms in graphene shown in Fig. 5(c) and (f) show that the above change of DOS comes from graphene for chemisorption and the isolated NO_2 molecule for physisorption. For other chemisorption and physisorption, there are similar properties.

Surprisingly, we can find interesting physical phenomena when analyzing the magnetic properties. First of all, graphene on O-terminated SiO_2 (100) substrate is non-magnetic, and spin polarization is introduced after the adsorption of the polarized NO_2 molecule. At first sight, the magnetic moments of all systems are the same as those of the isolated NO_2 molecule since the value is 1 μ_B. What is the difference of the magnetization here? For physisorption, the magnetization comes from the intrinsic spin polarization of an isolated NO_2 molecule. The difference of DOS between spin-up and spin-down electrons mainly comes from the C atoms and NO_2 molecule, as the analysis of the LDOS shown in Fig. 5. In order to give a clearer picture, the spin densities for typical chemisorption and physisorption are shown in Fig. 6. In agreement with the LDOS analysis, the spin density is mainly distributed on C atoms of graphene for chemisorption. This is different from the adsorption of molecule on doped graphene [9,12], where the spin density locates on the adsorbed molecules and doped atoms. More specifically, spin density locates in the C atoms with sp^2 hybridization. For C atoms forming covalent bonds with O atoms of SiO_2 substrate or N (O) atoms of NO_2 molecule, there is no unbonded electrons left, and therefore there is no spin polarization. It may be caused by the large charge transfer from graphene to the NO_2 molecule. By analyzing the Löwdin charge [46], 0.1808 e^- for "n" orientation and 0.2536 e^- for "o" orientation transfer from graphene to the NO_2 molecule on A site, spurring the rearranging of electrons in all C atoms. This is similar to the magnetic properties of graphene after the adsorption of H atoms [47], where the π bond in graphene was broken, and the unbonded electrons were redistributed. For physisorption, the unstable adsorption of NO_2 molecules concentrates all spin density, indicating the neglectable effect on the graphene system.

In the end, we investigate the possibility of the transition of configurations from physisorption to chemisorption reported above. After a Climbing-Image Nudged Elastic Band (CI-NEB) calculation, the minimum path from physisorption on B site to chemisorption on A site with "n" orientation is shown in Fig. 7, where five images are chosen in the calculation. It is shown that the barrier is about 0.05 eV. For other sites and other orientations, the barriers from physisorption to chemisorption are also below 0.1 eV, indicating the feasibility of the migration of molecules to stable chemisorption on graphene.

3.3. Van der Waals effect

In a lot of experiments, significant changes in conductivity and charge transfer are observed after the molecular adsorption even at room temperature [8,33], indicating the chemisorption should be dominant in the process. Since there is a barrier from physisorption to chemisorption here, we should ask what is the mechanism of inducing the final transition? The above results show that the barrier of 0.05 eV can be overcome by some external forces such as temperature of 580 K. However, it is well known that it cannot treat van der Waals interactions in DFT with GGA and LDA functional, which are also not included in the above calculations. Therefore, it is worthy understanding the van der Waals effect on the system. We firstly study the configurations of NO_2 on the pristine suspended graphene with van der Waals correction, resulting in similar physisorption except getting a little larger adsorption energies and smaller distances. Interestingly, after adding the correction term of DFT-D [43,44], the feature of physisorption on the graphene-SiO_2 system is totaly changed. Within van der Waals correction, the chemisorption of NO_2 on A site does not change. However, using the physisorption on B site as the initial configuration, the NO_2 molecule will diffuse without any barrier to chemisorption on A site. That is to say, the energy barrier from GGA calculation is a "pseudo barrier", and NO_2 on B site is not a stable configuration, which will transit to the stable one on A site. In other words, the van der Waals interactions between NO_2 and graphene "overcome" the barrier calculated from GGA functional. Thus, the mechanism of the experiments of graphene-SiO_2 system for the usage of gas

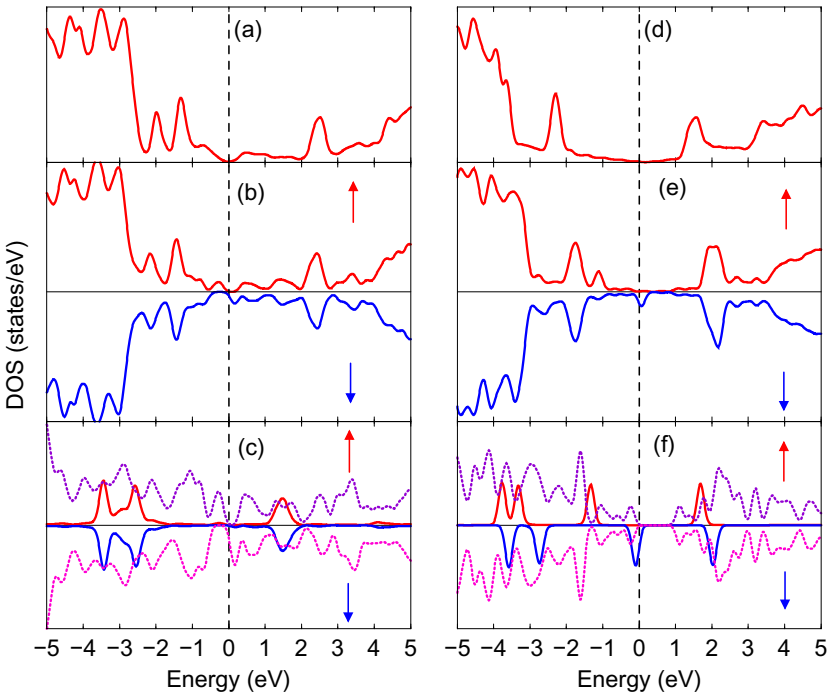

Fig. 5. (a) DOS of graphene-SiO_2 system with O-terminated surface, (b) DOS of adsorption of NO_2 on A site with "n" orientation, (c) LDOS of NO_2 (solid line) and carbon atoms in graphene (dotted line); (d)–(f) are the same as (a)–(c) with H-passivated surface. The orientation of arrows represents the direction of spin polarization. Dashed lines represent the Fermi level.

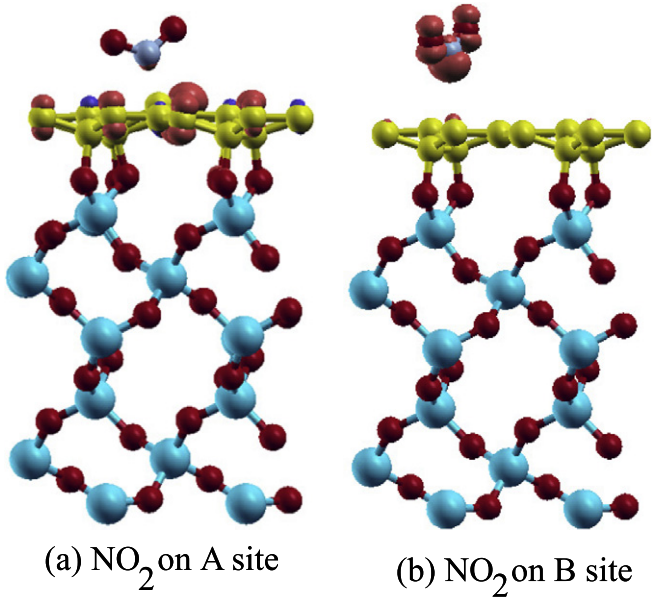

Fig. 6. (a) Spin density of "n" orientated NO_2 adsorption on A site; (b) Spin density of "n" orientated NO_2 adsorption on B site. Isosurface value is 0.01 a.u.

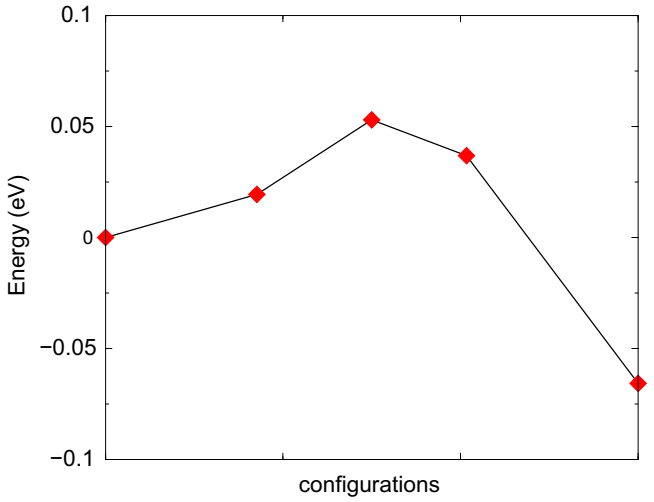

Fig. 7. Minimum energy pathways from B site to A site for NO_2 on graphene induced by SiO_2 substrate.

sensors with high sensitivity can be explained more clearly, leading to a good material for NO_2 sensors. In particular, the van der Waals attractions should be more important for the doping of molecules on mutilayer graphene [33], which can induce significant charge transfer between the graphene and the molecules.

3.4. Conclusion

In conclusion, the SiO_2 substrate and van der Waals interactions can enhance the detection of NO_2 molecule on graphene. The C–O covalent bonds and the local corrugations may be key reasons for this chemisorption. Furthermore, the chemisorption of NO_2 induces the visible change for the DOS around the Fermi level, which can be used as gas sensors with high sensitivity. Without van der Waals correction, the physisorption seems metastable with very small adsorption energy, and the change of DOS comes from the isolated-like NO_2 molecule. Interestingly, chemisorption of NO_2 on A site introduces spin polarization into graphene, and the intrinsic magnetization in NO_2 molecule disappears. Contrary to this, the magnetization of NO_2 retains its isolated characteristic for physisorption. Importantly, the "pseudo barrier" from physisorption to chemisorption transition with GGA calculation is only 0.05 eV and can be "overcome" by the consideration of the van

der Waals attraction. In fact, our further study shows that NH_3 on graphene-SiO_2 system has similar phenomena reported here, but the chemisorption is only the metastable configuration. This study explains well for the experiments of detecting NO_2 on graphene, and the system of graphene on SiO_2 surface with O-termination can also be used in the field of gas sensors and electronics.

Acknowledgments

We thank Professor Paolo Giannozzi (University of Udine) for helpful discussions. This work is supported by the National Natural Science Foundation of China under Grant Nos. 11104351 and 60921062. Funding support (SKLLIM1107) from the State Key Laboratory of Laser Interaction with Matter is acknowledged. Calculations are carried out at the Research Center of Supercomputing Application, NUDT.

References

[1] K.S. Novoselov, A.K. Geim, S.V. Morozov, D. Jiang, Y. Zhang, S.V. Dubonos, I.V. Grigorieva, A.A. Firsov, Science 306 (2004) 666.
[2] A.H. Castro Neto, F. Guinea, N.M.P. Peres, et al., Rev. Mod. Phys. 81 (2009) 109.
[3] F. Schedin, A.K. Geim, S.V. Morozov, E.W. Hill, P. Blake, M.I. Katsnelson, K.S. Novoselov, Nat. Mater. 6 (2007) 652.
[4] Md W.K. Nomani, R. Shishir, M. Qazi, D. Diwan, G. Koley, V.B. Shields, M.G. Spencer, G.S. Tompa, N.M. Sbrockey, Sensor. Actuat. B: Chem. 150 (2010) 301.
[5] H.E. Romero, P. Joshi, A.K. Gupta, H.R. Gutierrez, M.W. Cole, S.A. Tadigadapa, P.C. Eklund, Nanotechnology 20 (2009) 245501.
[6] J. Dai, P. Giannozzi, J. Yuan, Surf. Sci. 603 (2009) 3234.
[7] O. Leenaerts, B. Partoens, F.M. Peeters, Phys. Rev. B 77 (2008) 125416.
[8] T.O. Wehling, K.S. Noveselov, S.V. Morozov, E.E. Vdovin, M.I. Katsnelson, A.K. Geim, A.I. Lichtenstein, Nano. Lett. 8 (2008) 173.
[9] J. Dai, J. Yuan, P. Giannozzi, Appl. Phys. Lett. 95 (2009) 232105.
[10] I. Carrillo, E. Rangel, L.F. Magaña, Carbon 47 (2009) 2752.
[11] B. Sanyal, O. Eriksson, U. Jansson, H. Grennberg, Phys. Rev. B 79 (2009) 113409.
[12] J. Dai, J. Yuan, Phys. Rev. B 81 (2010) 165414.
[13] J. Dai, J. Yuan, J. Phys.: Condens. Matter 22 (2010) 225501.
[14] P.A. Denis, R. Faccio, A.W. Mombru, Chem. Phys. Chem. 10 (2009) 715.
[15] P.A. Denis, Chem. Phys. 353 (2008) 79.
[16] S. Tang, S. Zhang, Chem. Phys. 392 (2012) 33.
[17] Y. Lv, G. Zhuang, J. Wang, Y. Jia, Q. Xie, Phys. Chem. Chem. Phys. 13 (2011) 12472.
[18] Pablo A. Denis, J. Phys. Chem. C 115 (2011) 13392.
[19] A. Tapia, C. Acosta, R.A. Medina-Esquivel, G. Canto, Comput. Mater. Sci. 50 (2011) 2427.
[20] L.F. Huang, M.Y. Ni, G.R. Zhang, W.H. Zhou, Y.G. Li, X.H. Zheng, Z. Zeng, J. Chem. Phys. 135 (2011) 064705.
[21] S.Y. Zhou, G.H. Gweon, A.V. Fedorov, P.N. First, W.A. De Heer, D.-H. Lee, F. Guinea, A.H. Castro Neto, A. Lanzara, Nat. Mater. 6 (2007) 770.
[22] A. Mattausch, O. Pankratov, Phys. Rev. Lett. 99 (2007) 076802.
[23] V. Varchon, R. Feng, J. Hass, X. Li, B. Ngoc Nguyen, C. Naud, P. Mallet, J.-Y. Veuillen, C. Berger, E.H. Conrad, L. Magaud, Phys. Rev. Lett. 99 (2007) 126805.
[24] A. Ramasubramaniam, N.V. Medhekar, V.B. Shenoy, Nanotechnology 20 (2009) 275705.
[25] P. Shemella, S.K. Nayak, Appl. Phys. Lett. 94 (2009) 032101.
[26] Y.J. Kang, J. Kang, K.J. Chang, Phys. Rev. B 78 (2008) 115404.
[27] V. Geringer, M. Liebmann, T. Echtermeyer, et al., Phys. Rev. Lett. 102 (2009) 076102.
[28] Y. Shi, X. Dong, P. Chen, J. Wang, L.J. Li, Phys. Rev. B 79 (2009) 115402.
[29] M.Z. Hossain, Appl. Phys. Lett. 9 (2009) 143125.
[30] T.O. Wehling, A.I. Lichtenstein, M.I. Katsnelson, Appl. Phys. Lett. 93 (2008) 202110.
[31] S.Y. Zhou, D.A. Siegel, A.V. Fedorov, A. Lanzara, Phys. Rev. Lett. 101 (2008) 086402.
[32] C. Coletti, C. Riedl, D.S. Lee, B. Krauss, L. Patthey, K. von Klitzing, J.H. Smet, U. Starke, Phys. Rev. B 81 (2010) 235401.
[33] A.C. Crowther, A. Ghassaei, N. Jung, L.E. Brus, ACS Nano. 6 (2012) 1865.
[34] V.M. Bermudez, J.T. Robinson, Langmuir 27 (2011) 11026.
[35] J.P. Perdew, K. Burke, M. Ernzerhof, Phys. Rev. Lett. 77 (1996) 3865.
[36] The pseudopotentials of C.pbe-van_bm.UPF, O.pbe-van_bm.UPF, N.pbe-van_bm.UPF, H.pbe-van_bm.UPF, and Si.pbe-n-van.UPF are used in the website: <www.quantum-espresso.org>.
[37] P. Giannozzi et al. J. Phys.: Condens. Matter 21 (2009) 395502. URL: <www.quantum-espresso.org>.
[38] H.J. Monkhorst, J.D. Pack, Phys. Rev. B 13 (1976) 5188.
[39] M. Methfessel, A.T. Paxton, Phys. Rev. B 40 (1989) 3616.
[40] P.E. Blöchl, O. Jepsen, O.K. Andersen, Phys. Rev. B 49 (1994) 16223.
[41] M. Dion, H. Rydberg, E. Schröder, D.C. Langreth, B.I. Lundqvist, Phys. Rev. Lett. 92 (2004) 246401.
[42] G. Romn-Pérez, J.M. Soler, Phys. Rev. Lett. 103 (2009) 096102.
[43] V. Barone et al., J. Comput. Chem. 30 (2009) 934.
[44] S. Grimme, J. Comput. Chem. 27 (2006) 1787.
[45] D. Kang, J. Dai, Y. Hou, J. Yuan, J. Chem. Phys. 133 (2010) 014302.
[46] P.O. Löwdin, J. Chem. Phys. 18 (1950) 365.
[47] D.W. Boukhvalov, M.I. Katsnelson, A.I. Lichtenstein, Phys. Rev. B 77 (2008) 035427.